the binding of increasing number of ϵ-NAD^+ molecules. The latter mechanism has been previously proposed to explain CPL results of ϵ-NAD^+ which, like those of linear polarization presented here, change predominantly upon addition of the second coenzyme molecule.

The results obtained in the present study may be of a more general interest, since variation of p across single electronic bands may be more common than suspected. It was found before for the dansyl chromophore when bound to anti-dansyl antibodies.[19] Several more cases were listed elsewhere.[8] These results lead to some important conclusions. In the first place, whenever p varies across the emission band it is meaningless to present the excitation polarization spectrum without stating precisely what part of the emission band was used in the measurement. The variation of p in the fluorescence spectrum may explain in part why the limiting value of p expected to be 0.5 at the long-wavelength edge of the absorption spectrum is not often attained,[8] since it is common practice to collect a large part of the emission band in polarization studies. The sensitivity of p to the environment of the emitting chromophore in cases involving weak transitions dictates special precaution when p is used to probe the viscosity of the medium in which the chromophore is embedded, e.g., in membranes. If the transition is weak, changes in p may occur due to perturbation of the electronic levels rather than to changes in viscosity. Study of the polarization across the emission band may help verify the eligibility of a fluorophore for such purposes.

Finally it should be noted that fluorophores whose emission is due to a weak transition may be exploited to serve a useful purpose. The sensitivity of their polarization spectrum across the emission band to the environment of the fluorophore may be used as an additional property by which the environment is probed. Such an application of the emission polarization spectrum has been illustrated in the study of the heterogeneity of anti-dansyl anti-bodies.[19]

References and Notes

(1) J. A. Secrist, III, J. R. Barrio, and N. J. Leonard, *Science*, **175**, 646 (1972).
(2) J. R. Barrio, J. A. Secrist, III, and N. J. Leonard, *Proc. Natl. Acad. Sci. U.S.A.*, **69**, 2039 (1972).
(3) J. R. Barrio, J. A. Secrist, III, and N. J. Leonard, *Biochem. Biophys. Res. Commun.*, **46**, 597 (1972).
(4) J. A. Secrist, III, J. R. Barrio, N. J. Leonard, C. Villar-Palasi, and A. G. Gilman, *Science*, **177**, 279 (1972).
(5) J. A. Secrist, III, J. R. Barrio, N. J. Leonard, and G. Weber, *Biochemistry*, **11**, 3499 (1972).
(6) A. C. Albrecht, *J. Chem. Phys.*, **33**, 156 (1960).
(7) A. C. Albrecht, *J. Mol. Spectrosc.*, **6**, 84 (1961).
(8) I. Z. Steinberg in "Concepts in Biochemical Fluorescence", R. F. Chen and H. Edelhoch, Ed., Marcel Dekker, Vol. 1, New York, N.Y., 1975, p 79.
(9) J. Schlessinger, I. Z. Steinberg, and A. Levitzki, *J. Mol. Biol.*, **91**, 523 (1975).
(10) J. Schlessinger and A. Levitzki, *J. Mol. Biol.*, **82**, 547 (1974).
(11) H. Sund and H. Theorell in "The Enzymes", Vol. 7, P. D. Boyer, H. Lardy, and K. Myrback, Ed., Academic Press, New York, N.Y., 1963, p 26.
(12) S. F. Velick, *J. Biol. Chem.*, **233**, 1455 (1958).
(13) B. Ehrenberg, Ph.D. Thesis, The Weizmann Institute of Science, 1976.
(14) I. Z. Steinberg and A. Gafni, *Rev. Sci. Instrum.*, **43**, 409 (1972).
(15) G. Weber and B. Bablouzian, *J. Biol. Chem.*, **241**, 2558 (1966).
(16) A. Gafni in "Pyridine Nucleotide Dependent Dehydrogenases", Vol. 2, H. Sund, Ed., Walter de Gruyter, Berlin, 1977, p 237.
(17) P. L. Luisi, A. Baici, F. J. Bonner, and A. A. Aboderin, *Biochemistry*, **14**, 362 (1975).
(18) J. I. Harris and M. Waters in "The Enzymes", Vol. 13, P. D. Boyer, Ed., Academic Press, New York, N.Y., 1976, p 1.
(19) J. Schlessinger, I. Z. Steinberg, and I. Pecht, *J. Mol. Biol.*, **87**, 725 (1974).
(20) K. Mihashi and P. Wahl, *FEBS Lett.*, **52**, 8 (1975).
(21) More generally the dependence of the CPL on direction of the electric transition dipole moment will be minimal when the projection of the magnetic transition dipole moment on the plane defined by the rotating electric vector is parallel to the latter vector. Thus, the CPL may be unaffected by changes in the direction of the electric vector like those found in the present study (see Table I) even if the angle between the magnetic and electric vectors is large, as long as the general requirement stated above is fulfilled.

Electrochemistry of Vitamin B-12. 4. Kinetics and Mechanisms in B-12a–B-12r Oxido-Reduction

N. R. de Tacconi,[1a,b] D. Lexa,[1c] and J. M. Savéant*[1a]

Contribution from the Laboratoire d'Electrochimie de l'Université de Paris VII, 75 221 Paris Cedex 05, France, and the Laboratoire de Biophysique du Muséum d'Histoire Naturelle, 75 005 Paris, France.

Received February 28, 1978

Abstract: Cyclic voltammetry and rotating disk electrode voltammetry on gold, vitreous carbon, and mercury electrodes have been used to investigate the mechanism and the kinetic characteristics of B-12a–B-12r oxido-reduction. Base-on aquo-B-12a and base-on B-12r are the electrochemically reacting species in a large part of the pH range (pH 3–8), giving rise to a slow charge transfer. The charge transfer process involving the base-off forms is markedly more rapid. It begins to compete with the process involving the base-on forms only in very acidic media: below pH 1.5 for B-12r oxidation and below pH 0 for the reduction of B-12a. The nucleotide side-chain opening and closing rate constants have been derived from the evaluation of this competition. Above pH 8 two competing reduction processes are observed: reduction of the hydroxo form through its prior conversion into the aquo form and direct reduction of the hydroxo form. The latter, which completely predominates at pH 12, occurs at a potential negative to the B-12r–B-12s couple, giving rise to an apparent disproportionation phenomenon. The rate of proton abstraction from the aquo-B-12a yielding hydroxo-B-12a has been determined. A general picture summarizing the reaction pathways in the B-12a–B-12r–B-12s system and their thermodynamic and kinetic characteristics is given.

Decreasing from 3 to 1 the oxidation state of the cobalt atom in aquocobalamin, i.e., passing from B-12a to B-12r and B-12s, results in various changes in axial ligandations which are also under the dependence of the acidity of the medium. The equilibrium thermodynamics of these various reactions have been investigated in detail in the second paper of this series.[2] A quantitative description of the stability domains of the three oxidation states of cobalt in aquocobalamin as a function of potential and pH is thus available, providing the values of the characteristic standard potentials, pK_as, and equilibrium constants.

Regarding the B-12r–B-12s couple a kinetic investigation using cyclic voltammetry has provided a description of the oxido-reduction mechanisms at various pHs showing in par-

0002-7863/79/1501-0467$01.00/0

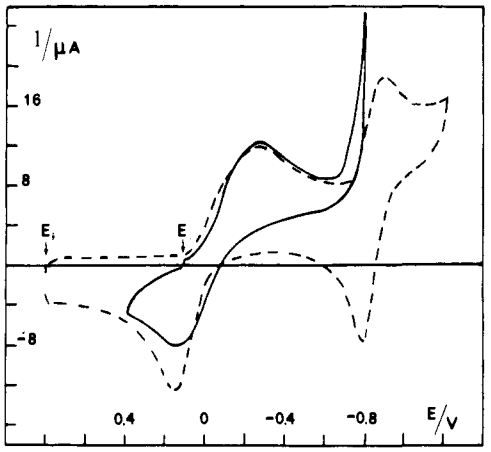

Figure 1. Cyclic voltammetry of the B-12a–B-12r system in neutral media: pH 4 (Britton–Robinson buffer), sweep rate 0.1 V s^{-1}, initial concentration 5×10^{-3} M. Full line: gold electrode. Dashed line: vitreous carbon electrode.

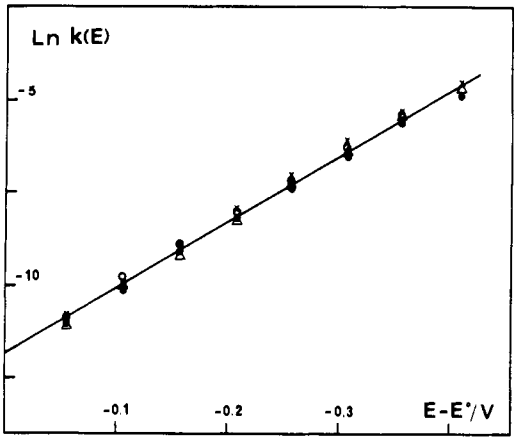

Figure 2. Rotating disk electrode voltammetry of the B-12a–B-12r system at pH 7 (Britton–Robinson buffer) on a gold electrode. Determination of the electron transfer rates at 125 (○), 250 (×), 500 (△), and 1000 (●) rev/min.

ticular the importance of the base-off–base-on reaction.[3] Several chemical and electrochemical characteristic rate constants were determined at this occasion. As far as kinetics and mechanisms are concerned no such investigation exists regarding the B-12a–B-12r system. Previous polarographic[4-6] and cyclic voltammetric[5] studies have been shown[2] to be uneasily interpretable owing to the probable interference of mercury oxidation. So far, the only available kinetic data on the B-12a–B-12r oxido-reduction is merely the indication that, on a gold electrode, the system is much slower than the B-12r–B-12s couple, particularly in alkaline media.[2]

In the present paper we attempt to provide a detailed description of the kinetics and mechanisms in the B-12a–B-12r system as a function of pH. Based on the previous thermodynamic analysis of this system[2] it can be predicted that the pH range will be divided into three main regions according to the nature of the accompanying ligand exchange reactions: (1) neutral media (pH 3–8), both members of the electrochemical couple are base-on forms; (2) alkaline media (pH >8), interference of the hydroxo form of B-12a; (3) acidic media (pH <3), interference of the side-chain opening reactions first at the Co(II) and then at the Co(III) level.

Several electrode materials were employed depending on medium acidity. In neutral media both gold and vitreous carbon were used. Vitreous carbon was mostly used in the most acidic media since the potential for hydrogen evolution is markedly more negative than with gold. In alkaline media a gold electrode was generally employed. However, a few experiments were carried out with mercury at the highest pH since the B-12a wave is then sufficiently negative to be clearly out of any interference with mercury oxidation. Two techniques were employed: cyclic voltammetry (CV) and rotating disk electrode voltammetry (RDEV).

Results

Neutral Media. CV and RDEV experiments were carried out on a gold electrode at several pHs ranging from 3 to 8. A typical cyclic voltammogram obtained at pH 4 is represented in Figure 1 showing two waves with the first markedly less reversible than the second. Accordingly, two waves of equal heights are observed in RDEV corresponding to B-12a → B-12r and B-12r → B-12s reductions, respectively.

The first cathodic wave apparently features a simple slow electron transfer process with negligible influence of associated chemical reactions.[7-9] This would correspond to the reduction of base-on B-12a into base-on B-12r (reaction e1 on the mechanistic chart below), which are the stable species in the considered pH range.[2] It also implies that the most probable loss of a water molecule in the sixth axial coordination is so rapid that it can be considered as a part of the charge transfer rather than a pre- or a postassociated chemical reaction. On these grounds the kinetic characteristics, transfer coefficient (α_1), and standard rate constant ($k_S^{ap,1}$) can be derived from the analysis of the RDEV waves[10] taking for the standard potential the value (−0.042 V vs. SCE) obtained from previous spectroelectrochemical experiments[2] and for the diffusion coefficient $D = 1.5 \times 10^{-6}$ cm^2 s^{-1} (see Experimental Section). The results of such an analysis are shown in Figure 2 for 4 rotation speeds at pH 7 under the form of a ln $k(E)$ vs. $(E - E_1^0)$ plot with

$$k(E) = k_S^{ap,1} \exp[-\alpha_1(F/RT)(E - E_1^0)]$$

being obtained from

$$\ln [k(E)] = \ln (D/\delta) - \ln \left\{\frac{i_l - i\{1 + \exp[-\alpha_1(F/RT)(E - E_1^0)]\}}{i}\right\}$$

(i_l = limiting current; δ = diffusion layer thickness; here δ(cm) $= 3.4 \times 10^{-3}\, \omega_{(H)}^{-1/2}$).

The average values of α_1 and $k_S^{ap,1}$ are given in Table I. It is seen that they practically do not depend upon pH and on the medium being buffered or not. This shows that eventual replacement of water by an anion of the buffer as sixth ligand exerts no significant influence on the characteristics of the charge transfer reaction.

The voltammograms obtained on gold and on vitreous carbon at the same pH (Figure 1) exhibit very little difference. This leads to the important conclusion that the above charge transfer constants reflect the intrinsic properties of the reduction of base-on B-12a into base-on B-12r with negligible influence of the electrode material. On the average, $\alpha_1 = 0.46$, $k_S^{ap,1} = 8 \times 10^{-6}$ cm s^{-1}, $E_1^0 = -0.042$ V vs. SCE.

Table I. Characteristics of Base-on B-12a–Base-on B-12r Oxido-Reduction

pH	E_1^0, V vs. SCE	α_1	$k_S^{ap,1}$, cm s^{-1}	D, cm^2 s^{-1}
4[a]	−0.050	0.48	7.3×10^{-6}	1.9×10^{-6}
6.3[b]	−0.050	0.45	8.3×10^{-5}	2.2×10^{-6}
7[a]	−0.040	0.45	7.5×10^{-6}	1.9×10^{-6}
av	−0.047	0.46	8×10^{-6}	2×10^{-6}

[a] Britton–Robinson buffer. [b] ClO_4Na 0.05 M.

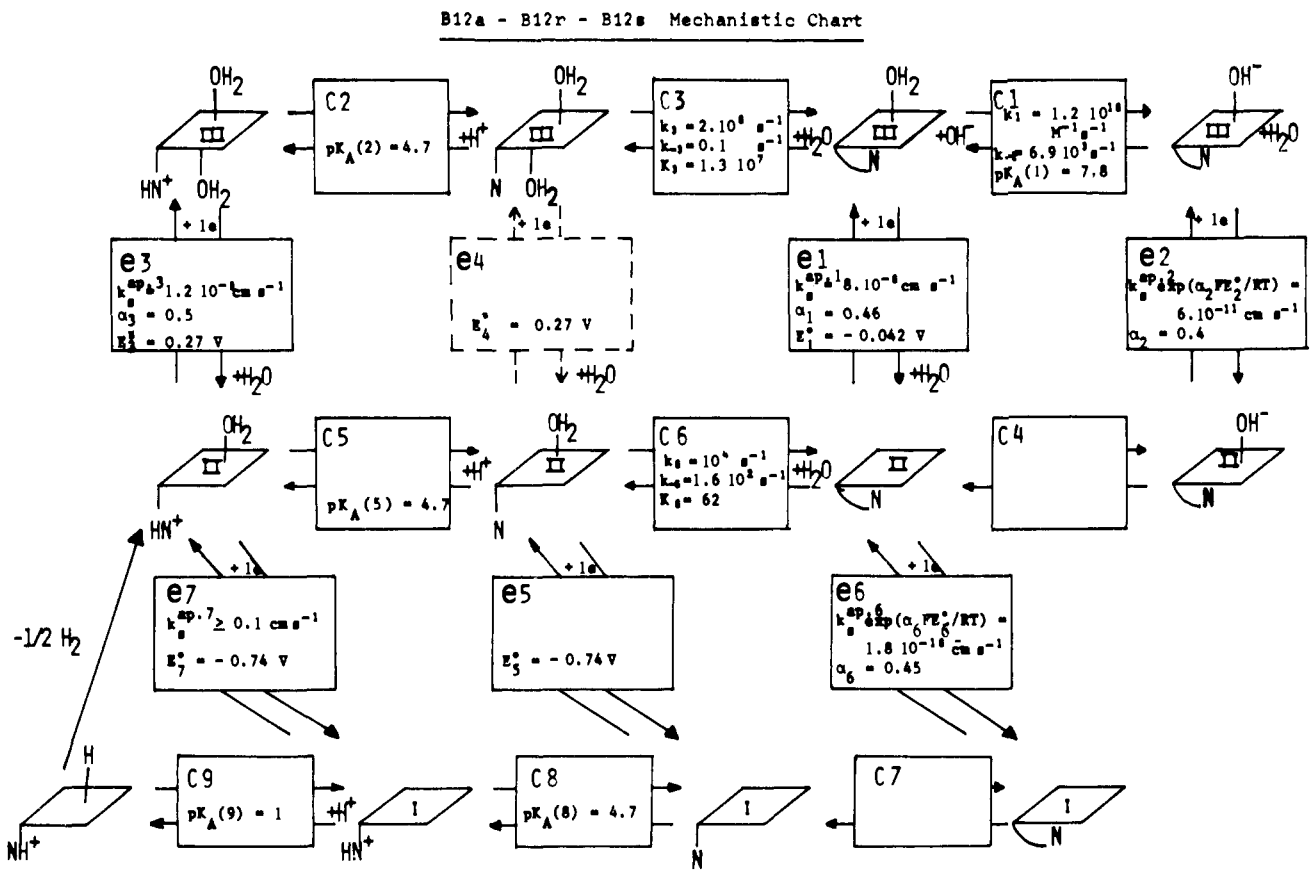

The anodic peak is such that the middle between its position and that of the cathodic peak gives an E_1^0 value (second column of Table I) very close to the spectroelectrochemical value. The agreement between these E^0 determinations and the spectroelectrochemical data suggests that oxidation of B-12r into B-12a follows in the reverse direction the same pathway as the reduction, i.e., involves the base-on forms only. This point will be confirmed by the results obtained in acidic media which are reported below. They show that oxidation of B-12r involves the base-on form down to pH 1.5. In the last column of Table I are figured values of the diffusion coefficient as derived from the height of the RDEV wave[10] using the geometrical surface area of the disk. It is seen that they are slightly larger than the value determined below as can be expected from the actual surface area of the electrode being larger than its geometrical surface area.

Alkaline Media. Above pH 8, the hydroxo form of B-12a tends to predominate over the aquo form at equilibrium.[2] This results first in a negative shift of the CV peak potential (Figure 3) and of the RDEV half-wave potential (Figure 4) with pH. Then, while still moving negatively, the first wave decreases at the expense of the second wave. That the sum of the two wave heights remains constant and corresponds to an overall electron exchange of 2 faradays/mol is clearly seen on the RDE voltammograms (Figure 4). It is noted that, when sufficiently small, the height of the first wave varies with the rotation speed ω much less than proportionally to $\omega^{1/2}$ as would be the case for a diffusion-controlled process. This behavior is typical, at the level of the first wave, of a reaction sequence involving a chemical reaction preceding a charge-transfer process.[11] The height of the first wave reflects then the kinetics and thermodynamics of the antecedent chemical reaction while the location of the wave depends upon these parameters as well as upon the charge-transfer kinetics. The aquo form being easier to reduce than the hydroxo form, it follows that the first cathodic wave features the reduction of B-12a through its aquo

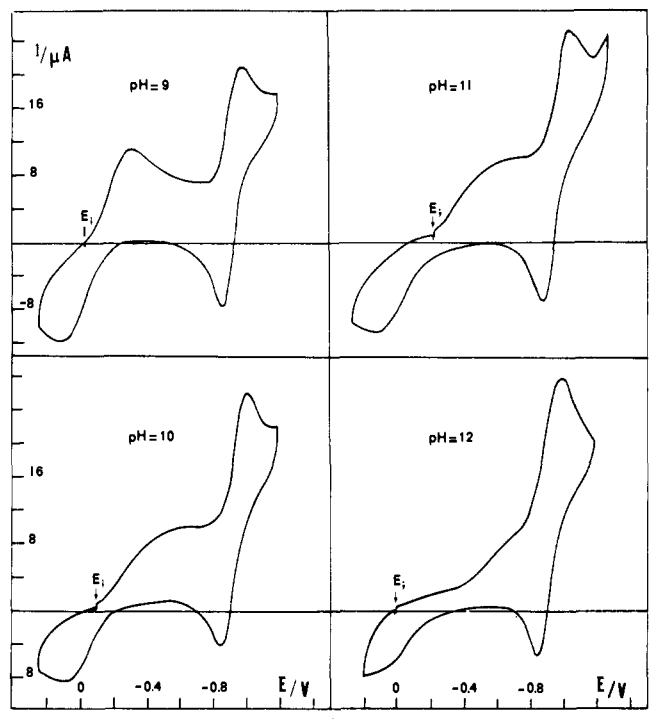

Figure 3. Cyclic voltammetry of the B-12a–B-12r system in alkaline media on a gold electrode: sweep rate 0.1 V s^{-1}, B-12 concn 5 × 10^{-3} M.

form (reaction path (c1 + e1) on the chart). On these grounds, the rate constants k_1 and k_{-1} can be derived from the height of the first cathodic RDEV wave according to[12]

$$i_l/(i_l)_d = K\lambda^{1/2}/(K\lambda^{1/2} + 1)$$

i_l being the observed limiting current and $(i_l)_d$ the diffusion-controlled limiting current. K is the equilibrium constant of

Table II. RDEV Determination of the Rate Constant of the Reaction Aquo-B-12a ⇄ Hydroxo-B-12a

ω, rev/min	pH 10		pH 11		pH 12	
	$i_l/(i_l)_d$	$(k'_1 + k'_{-1})$, s^{-1}	$i_l/(i_l)_d$	$(k'_1 + k'_{-1})$, s^{-1}	$i_l/(i_l)_d$	$(k'_1 + k'_{-1})$, s^{-1}
125			0.87	2.8×10^7	0.58	1.3×10^8
250	0.89	9.2×10^5	0.79	1.9×10^7	0.49	1.3×10^8
500	0.82	5.8×10^5	0.70	1.5×10^7	0.43	1.5×10^8
1000	0.75	4.7×10^5	0.62	1.4×10^7	0.34	1.5×10^8
2000	0.72	7.1×10^5				
av		6.5×10^5		1.6×10^7		1.4×10^8

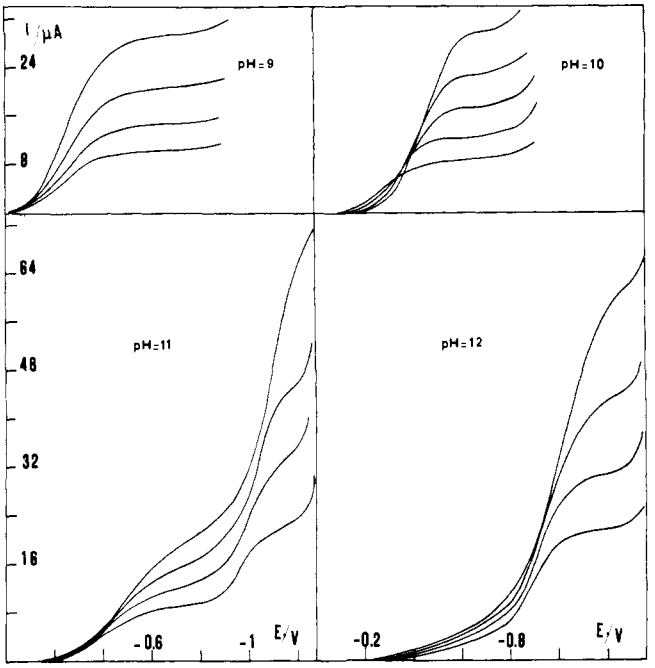

Figure 4. Rotating disk electrode voltammetry of the B-12a–B-12r system in alkaline media on a gold electrode. Rotation speed: 125, 250, 500, 1000, and 2000 rev/min. B-12 concn: 5×10^{-3} M.

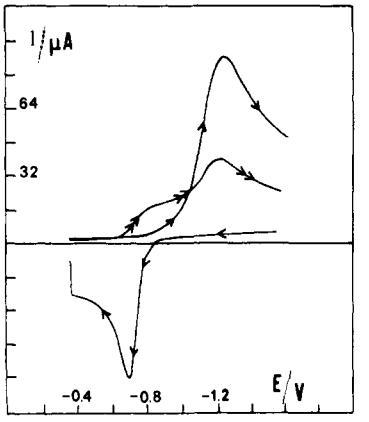

Figure 5. Cyclic voltammetry of the B-12a–B-12r system on a mercury electrode at pH 12 (Britton–Robinson buffer with 0.1 M tetrabutylammonium *p*-toluenesulfonate): sweep rate 13 V s^{-1}, B-12 concn 2.4×10^{-3} M.

the antecedent reaction:

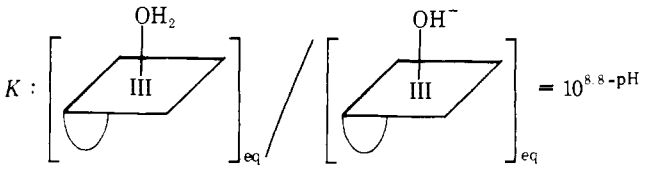

λ is a kinetic factor comparing the rate of the chemical reaction to the rate of diffusion

$$\lambda = (k'_1 + k'_{-1})\delta^2/D$$

k'_1 and k'_{-1} being the pseudo-first-order rate constants of reaction c1. The results are shown in Table II for three pH values. Assuming the proton abstraction in the sixth ligand water molecule to be operated by OH, the second-order rate constant k_1 is found as equal to 6.5×10^9, 1.6×10^{10}, and 1.4×10^{10} M^{-1} s^{-1} at pH 10, 11, and 12 respectively, i.e., satisfactorily constant within experimental error.

As can be seen in Figures 3 and 4, the second wave features the direct reduction of the hydroxo form, which occurs at a potential very close to the reversible reduction potential of B-12r into B-12s. The same is found at pH 12 on a mercury electrode. Indeed, at this pH, the first wave becomes unimportant provided that the sweep rate is sufficiently high (Figure 5). The second wave is then negative enough to be recorded without interference of mercury oxidation. It is interesting to note that the reduction wave of the hydroxo-B-12a is now clearly negative to the reversible potential of the B-12r–B-12s couple. This is related to the fact that the electron transfer to hydroxo-B-12a is slow and that the sweep rate is higher (13 V s^{-1}) than in the above experiments on a gold electrode. The anodic wave in Figure 5 has been recorded starting from negative potentials in order for its height to be directly compared to that of the cathodic wave. The peak width of the cathodic wave indicates that the transfer coefficient for the reduction of hydroxo-B-12 is $\alpha_2 = 0.4$.[7] With this value of α the height of the cathodic wave should be 1.3 times that of the anodic wave.[7] This figure is indeed found by direct comparison of the cathodic and anodic peak heights in Figure 5. Direct electron transfer to hydroxo-B-12a leads to a B-12r with an OH^- as sixth ligand. This is obviously an extremely unstable species which immediately decomposes into the standard base-on B-12r which is reduced into B-12s at this potential. Accordingly no trace of reversibility could be found even raising the sweep rate up to 1400 V s^{-1}. During a second cathodic scanning the characteristic pattern of B-12r is found in place of the initial wave (compare the present Figure 5 with Figure 5a in ref 3). It follows that the standard potential of reaction e2 cannot be determined and so for the standard rate constant. The only attainable kinetic characterization of this electron transfer process is therefore the forward rate constant:

$$k_S^{ap,2} \exp(\alpha_2 F E_2^0/RT) = 6 \times 10^{-11} \text{ cm s}^{-1}$$

Turning back to cyclic voltammetry on gold, it was observed that the peak potential of the anodic wave featuring the reoxidation of B-12r into B-12a practically does not vary with pH between 9 and 11 and has about the same value (+0.13 V vs. SCE) as in neutral media. This is in accordance with the oxidation of B-12r following the pathway (e1) + (c1). In such conditions, the deprotonation reaction has indeed no influence

Table III. CV Determination of the Rate Constants of the B-12a Base-off-Base-on Reaction

v, V s^{-1}	pH 0 ($K = 4 \times 10^{-3}$) $i_p/(i_p)_d$	λ	$(k_f + k_b)$, s^{-1}	$H_0 = -1$ ($K = 4 \times 10^{-2}$) $(i_p/(i_p)_d$	λ	$(k_f + k_b)$, s^{-1}
0.05	0.054	21.4	43	0.080	1.0	2
0.10	0.038	10.0	40	0.075	0.7	3
0.20	0.036	6.3	50	0.056	0.5	4
av	$k_b = 44$; $k_f = k_{-3} = 0.18$; $k_3 = 2.2 \times 10^6$			$k_b = 3$; $k_f = k_{-3} = 0.12$; $k_3 = 1.5 \times 10^6$		

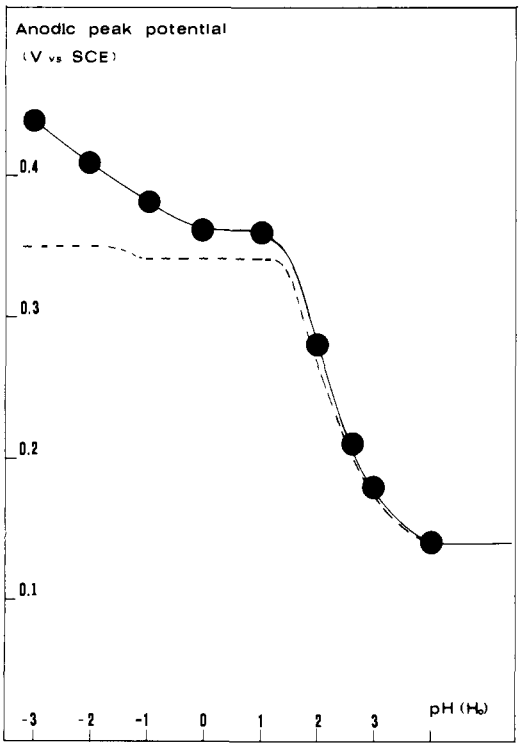

Figure 6. Cyclic voltammetry of the B-12a–B-12r system on a vitreous carbon electrode in acidic media. Anodic peak potential as a function of pH: B-12 concn 4×10^{-3} M, sweep rate 0.1 V s^{-1}. Full line: experimental. Dashed line: theoretical.

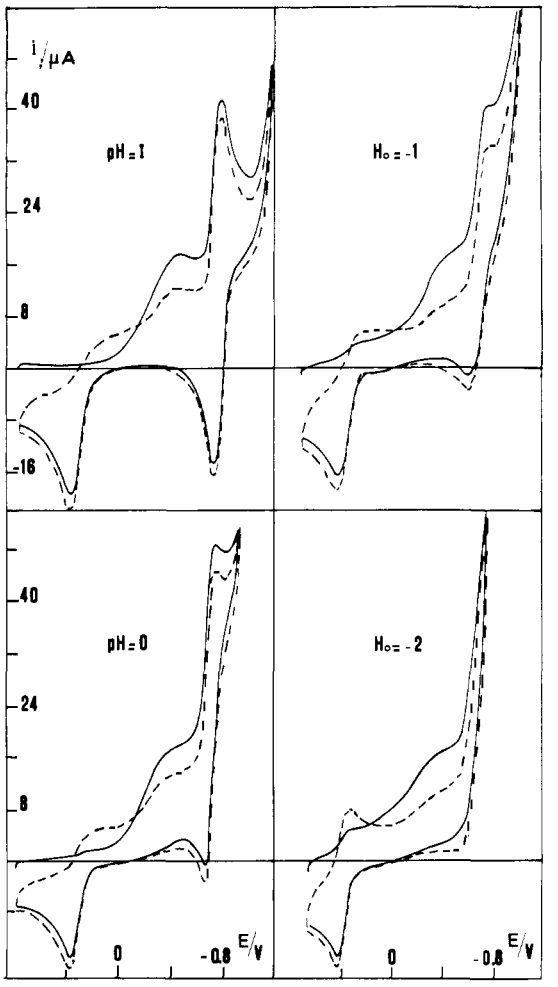

Figure 7. Cyclic voltammetry of the B-12a–B-12r system on a vitreous carbon electrode at pH (H_0) = 1, 0, −1, −2: sweep rate 0.1 V s^{-1}, B-12 concn 4×10^{-3} M. Full line: first sweep. Dashed line: second sweep.

on the overall kinetics, the electron transfer step being rate determining.

Acidic Media. A vitreous carbon electrode was used systematically in acidic media for the reasons given previously.

The first modification which is observed when the pH is decreased below 3 is a positive shift of the anodic peak (Figure 6). The cathodic pattern remains unchanged down to pH 0. At this pH, a small prewave appears on the first cathodic scan, its height being approximately independent of the sweep rate. The height of this prewave increases when the pH decreases (Figure 7). During a second cathodic scan the height of the prewave is higher than during the first. An almost reversible system is thus obtained at $H_0 = -2$ (the Hammett acidity function H_0[13] is used instead of pH below pH 0).

The appearance of the prewave is typical of a reaction sequence involving a chemical reaction preceding the electron transfer process.[11] This suggests that below pH 0 a part of the reduction occurs through the protonated base-off B-12a, although the less reducible base-on B-12a predominates at equilibrium in this pH range. It leads to protonated base-off B-12r which is then the stable form of B-12r. The rate constants of the base-off reaction can be derived from the height of the prewave.[11] The results are shown in Table III for three sweep rates at pH 0 and −1. k_f and k_b are the rate constants for the formation of the protonated base-off and base-on B-12a, respectively. $K = k_f/k_b$ is the equilibrium constant corresponding to the formation of the protonated B-12a ($K = 10^{pK_A - pH}$). The calculations are dependent upon the value of the pK_A. We took −2.4 as determined previously by spectrophotometry[14] and which corresponds to an E^0 for the base-off B-12a–base-off B-12r couple of 0.27 V vs. SCE.[2] A confirmation that this pK_A value is correct is provided by the E^0 of the aquocob(II)-inamid couple being 0.26 V vs. SCE.[15]

It is seen in Table III that k_f does not vary with pH whereas k_b decreases with pH by a decade per pH unit. This in accordance with a base-on–base-off conversion involving first the opening of the nucleotide side chain and then the protonation of Bzm rather than a direct attack of the proton on the Bzm nitrogen bonded to the cobalt. In the latter case, indeed, k_f should increase with acidity and k_b remain constant. In the context of the first mechanism (c2 + c3 on the chart) reaction c2 can be regarded as being always equilibrated since k_2 and

k_{-2} are large as compared to k_3 and k_{-3}. Thus $k_3 = k_b(1 + 10^{4.7-pH})$ and $k_{-3} = k_f$.

In agreement with this (c2 + c3) mechanism, k_3 and k_{-3} are found satisfactorily constant when the pH varies (Table III).

The kinetic characteristics of the base-on B-12a–base-on B-12r electron transfer (e3) can be derived from the quasi-reversible voltammogram obtained at $H_0 = -2$ and the width of the anodic peak at higher pHs (Figure 7). At, e.g., pH 1 the rate of reaction (c2 + c3) following the charge transfer (e3) is sufficient to render the system completely irreversible (see Figure 1 in ref 9 with $\log \Lambda = -0.37$ and $\log \lambda = 2$). The peak width then leads to $\alpha_3 \simeq 0.5$. Analysis[11] of the quasi-reversible pattern obtained at $H_0 = -2$ then gives

$$k_S^{ap,3} = 1.2 \times 10^{-3} \text{ cm s}^{-1}$$

Similar values are found for the cob(III)inamid/cob(II)inamid couple.[15] However, when decreasing the pH below −1 a positive shift of the anodic peak potential is observed reflecting a similar variation of the base-off B-12a–base-off B-12r standard potential. This may reflect a further protonation reaction involving the base-off B-12r.

The positive shift of the anodic peak between pH 3 and 1 can be interpreted as follows. The base-on B-12r is easier to oxidize than the protonated base-off form. At 0.1 V s^{-1} base-on B-12r oxidation corresponds to an irreversible peak potential at 0.14 V whereas the irreversible peak of base-off B-12r is located at 0.34 V. In the last case the follow-up chemical reactions (c2 + c3) are so fast that the rate-determining step is indeed the charge transfer as it is in the first case. However, when decreasing the pH below 2.9 the proportion of base-on form at equilibrium decreases:

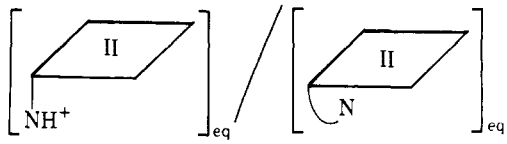

$$= 10^{-1.8} + 10^{2.9-pH}$$

Then the peak potential of base-on B-12r oxidation is given by

$$E_p^a = 0.14 + (0.059/\alpha_1) \log (1 + 10^{-1.8} + 10^{2.9-pH})$$

The resulting variations of the anodic peak with pH are represented in Figure 7 (dashed lines). It is seen that the value of 0.34 is reached at about pH 1.5. It follows than between pH 3 and 1.5 the most oxidizable form of B-12r remains the base-on form. Along the anodic wave, oxidation thus proceeds first via the base-on B-12r (reaction e1) and then involves the protonated base-off form beyond 0.34 V. Between pH 3 and 1.5 the sum of the nucleotide side-chain opening and closing rate constants is about 160 s^{-1}.[3,16] At low sweep rates as used here, these reactions do not therefore influence the overall kinetics, the base-off–base-on reaction remaining at equilibrium.[11] This explains why no splitting of the anodic wave is observed with a first part that would correspond to the oxidation of the base-on form and a second part to the base-off form.

Discussion

The various possible reduction and oxidation pathways and the corresponding thermodynamic and kinetic constants have been discussed above following the description of the experimental results. It is, however, necessary to further discuss a few points.

From the results obtained in acidic media it is now possible to evaluate the influence of the base-on–base-off reaction in the reduction of B-12a in neutral media. In the antecedent base-off–base-on reaction (c2 + c3) the overall closing rate constant is

$$k_b = 2 \times 10^6/(1 + 10^{4.7-pH})$$

The equilibrium constant of the opening reaction being

$$K = 10^{-2.4-pH}$$

with = $(RT/F)(k_b/v)$, the height of the kinetic wave corresponding to the reduction through the base-off form as compared to a diffusion-controlled wave is[14]

$$(i_p)/(i_p)_d = K\sqrt{\lambda}/0.446$$

This ratio is given as a function of pH in Table IV for a low sweep rate, 0.1 V s^{-1}. It is seen that, above pH 3, this reduction pathway is completely negligible as compared to the direct reduction of the base-on form.

Table IV. Reduction of the Base-off Form in Neutral Media as Compared to the Reduction of the Base-on Form

pH	K	k_b, s^{-1}	λ	$(i_p)/(i_p)_d$
3	4×10^{-6}	4×10^4	10^4	9×10^{-4}
4	4×10^{-7}	4×10^5	10^5	3×10^{-4}
5	4×10^{-8}	1.3×10^6	3.3×10^5	5×10^{-5}
6	4×10^{-9}	1.9×10^6	4.8×10^5	6×10^{-6}
7	4×10^{-10}	2×10^6	5×10^5	6×10^{-7}

From the single two-electron wave obtained in very alkaline medium (pH ≥12) one might infer that B-12r is able to disproportionate into B-12a and B-12s. It has been shown,[2] on the basis of equilibrium measurements, that this is actually not true, even though the disproportionation equilibrium constant tends to increase somewhat at high pH. The disproportionation-like behavior actually results from kinetic factors, both chemical and electrochemical. The first of these is that the conversion of the aquo form into the hydroxo form is slower and slower as the pH increases resulting in a reduction pathway involving only the latter. On the other hand, electron transfer to the hydroxo-B-12a is slow thus arising at a potential negative to the B-12r–B-12s couple which results in a two-electron wave.

It is interesting to note the large differences in the standard rate constants of electron transfer to the various forms of the B-12 species. Electron transfer to base-on B-12a is 150 times slower than to base-off B-12a. This seems to be related to Bzm being more strongly bonded to the cobalt atom than water, which results in a larger vibrational contribution to the reorganization energy of the electron transfer.[17,18] Similarly, electron transfer is much faster in the base-off B-12r–base-off B-12s couple ($k_S \geq 0.1$ cm s^{-1})[3] than in the base-off B-12a–base-off B-12r couple ($k_S = 2 \times 10^{-3}$ cm s^{-1}) reflecting a smaller change in the vibrational energy in the first case than in the second.

In conclusion, the mechanism of the B-12a–B-12r oxido-reduction can be summarized as a function of pH and potential along the following lines:

(1) Reduction of B-12a occurs via the aquo-base-on form in the largest part of the pH range (1–8).

(2) Between pH 3 and 8 it involves a simple charge transfer (reaction c1) whereas at pH 3 the base-on B-12r initially formed is converted into its protonated base-off form.

(3) Base-off B-12a begins to interfere noticeably only below pH 1 (reaction path: c3 + c2 + e3), a part of the reduction still occurring through the base-on form (e1 + c6 + c5) at a more negative potential. Very acidic media ($H_0 < -2.4$) are required in order that this last route becomes negligible.

(4) Oxidation of B-12r into B-12a involves the base-on form above pH 3 (reaction e1). It occurs exclusively through the base-off form only below pH 1.5. Between these two pHs both routes are followed depending upon potential.

(5) In alkaline media, a part of the reduction whose importance decreases when raising pH still occurs through the aquo-base-on B-12a (c1 + e1) up to pH 12. The remainder of the current involves the reduction of the hydroxo form, which requires a more negative potential (e2) and leads directly B-12s in a two-electron process.

In the above mechanistic chart are also figured the results previously obtained for the B-12r–B-12s system[3] so as to present a general picture of the reaction pathways and their thermodynamic and kinetic characteristics[19] for the three oxidation states of aquocobalamin.

Experimental Section

Chemicals. Both acetatocobalamin (Rhône-Poulenc) and hydroxocobalamin (Roussel-Uclaf) were used in buffered media while only the first was used for the experiments in unbuffered media. Britton-Robinson buffers and perchloric acid solutions below pH 2 were employed as described in ref 3. In unbuffered solutions the supporting electrolyte was sodium perchlorate in 0.05 M concentration. All the solutions were prepared from water distilled twice in a quartz apparatus. The B-12 concentration was 5×10^{-3} M L^{-1}.

Cyclic Voltammetry and Rotating Disk Electrode Voltammetry. The instrumentation, cell and electrodes, and mercury working electrode were the same as in ref 2. The rotation system was from Tacussel (EDI + CONTROVIT). The gold and vitreous carbon electrodes were disks of 3×10^{-2} and 7×10^{-2} cm^2 geometrical surface area, respectively. Both electrodes were polished with diamond paste of decreasing particle size (7, 3.5, and 1 μ) between each run in RDEV and every ten runs in CV. After polishing the gold electrode was rinsed with acetone and water successively and the carbon electrode with water and methanol. Reproducible results were thus obtained both in blank experiments and in the presence of B-12.

Determination of the Diffusion Coefficient. Previous determinations[4] have led to the value of 4×10^{-6} cm^2 s^{-1} that we have used previously in our kinetic analysis of the B-12r–B-12s system.[3] Since in the present investigation the value of the diffusion coefficient is repeatedly required for determining charge transfer and chemical reaction rate constants we have tried to check the above-mentioned value. Two methods were employed in this purpose. The first one is based on cyclic voltammetry of the B-12r–B-12s system in acidic medium ($HClO_4$ 0.1 M) on a hanging mercury drop electrode of known surface area. In these conditions the electrochemical process simply involves a fast charge transfer with no detectable interference of associated chemical reactions and of reactant adsorption.

The results are shown in Figure 8 under the form of a plot of peak current vs. square root of sweep rate. From the slope of this plot the diffusion coefficient is found[7] as equal to 1.4×10^{-6} cm^2 s^{-1}, i.e., markedly smaller than the previous value. We then employed the capillary method[20,21] starting from aquocobalamin 2×10^{-3} M in 0.02 M KCl. After 5 days the concentration was decreased by a factor of 0.66 as determined by UV–visible spectrophotometry which led to $D = 1.6 \times 10^{-6}$ cm^2 s^{-1} In the analysis described so far we have therefore used $D = 1.5 \times 10^{-5}$ cm^2 s^{-1}. The value determined by the Stokes method[4] may have been in error since the method is not well adapted to concentrations at the millimolar level.[22]

Acknowledgment. This work was supported in part by the Centre National de la Recherche Scientifique (Equipe de Recherche Associée 309 "Electrochimie Moléculaire"). We thank the Conseijo Nacional de Investigaciones Cientificas y Tecnicas de la Republica Argentina for having provided a postdoctoral fellowship to one of us (N. R. de Tacconi). The Roussel-Uclaf Co. and the Rhone-Poulenc Co. are thanked for the gift of aquo- and acetatocobalamin samples. We are grateful to Professor R. Gross (Strasbourg, France) for helpful advice regarding the carbon electrode polishing procedures and for the gift of a vitreous carbon rod. Thanks are also due to Professor M. Chemla (Laboratoire d'Electrochimie de l'Université de Paris VI, France) for helpful advice in the determination of diffusion coefficients by the capillary method and Miss Roumegous for her technical assistance in these measurements.

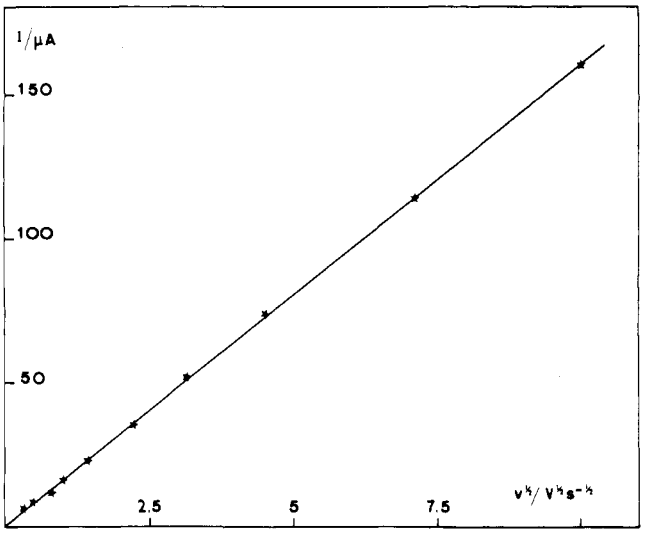

Figure 8. Determination of the diffusion coefficient from cyclic voltammetry of B-12r in 0.1 M $HClO_4$: B-12 concn 2×10^{-3} M, electrode surface area 0.0267 cm^2.

References and Notes

(1) (a) Laboratoire d'Electrochimie de l'Université de Paris VII; (b) Instituto de Investigaciones Fisicoquimicas Teoricas y Aplicadas-Sucursal 4, C.C. 16, 1900 La Plata, Argentina; (c) Laboratoire de Biophysique du Muséum d'Histoire Naturelle.
(2) D. Lexa, J. M. Savéant, and J. Zickler, *J. Am. Chem. Soc.*, **99**, 2786 (1977).
(3) D. Lexa and J. M. Saveant, *J. Am. Chem. Soc.*, **98**, 2652 (1976).
(4) H. P. C. Hogenkamp and S. Holmes, *Biochemistry*, **9**, 1886 (1970).
(5) R. L. Birke, G. A. Brydon, and M. F. Boyle, *J. Electroanal. Chem.*, **52**, 237 (1974).
(6) T. M. Kenyhercz and H. B. Mark Jr., *Anal. Lett.*, **7**, 1 (1974).
(7) H. Matsuda and Y. Ayabe, *Z. Elektrochem.*, **59**, 494 (1955).
(8) R. S. Nicholson, *Anal. Chem.*, **37**, 1351 (1965).
(9) L. Nadjo and J. M. Saveant, *J. Electroanal. Chem.*, **48**, 113 (1973).
(10) J. Albery, "Electrode Kinetics", Clarendon Press, Oxford, 1975.
(11) J. M. Saveant and E. Vianello, *Electrochim. Acta*, **8**, 905 (1965).
(12) F. Opekar and P. Beran, *J. Electroanal. Chem.*, **69**, 1 (1976).
(13) C. H. Rochester, "Organic Chemistry", Vol. 17, A. T. B. Blomquist and H. A. Wasserman, Ed., Academic Press, New York, N.Y., 1970.
(14) G. C. Hayward, H. A. O. Hill, J. M. Pratt, N. J. Vanston, and R. J. P. Williams, *J. Chem. Soc.*, 6485 (1965).
(15) N. R. de Tacconi, D. Lexa, J. M. Savéant, and J. Zickler, to be published.
(16) The intrinsic rate constants for the side-chain opening and closing in B-12r are 1.6×10^2 and 10^4 s^{-1}, respectively, and not 1.6×10^3 and 10^5 s^{-1} as reported in ref 3 due to a transcription error.
(17) R. A. Marcus in "Dalhem Workshop on the Nature of Seawater, Dalhem Konferenzen", E. D. Goldberg, Ed., Abakon Verlagsgesellschaft, West Berlin, 1975, pp 477–504.
(18) J. M. Hale in "Reactions of Molecules at Electrodes", N. S. Hush, Ed., Wiley-Interscience, New York, N.Y., 1971, pp 229–257.
(19) The forward rate constant of electron transfer e6 has been corrected taking into account the new value of the diffusion coefficient determined as described in the Experimental Section.
(20) J. S. Anderson and K. Saddington, *J. Chem. Soc.*, 538 (1949).
(21) P. Turq, F. Lantelme, Y. Roumegous, and M. Chemla, *J. Chim. Phys. Phys.-Chim. Biol.*, 681 (1972).
(22) R. A. Robinson and R. H. Stokes, "Electrolyte Solutions", Butterworths, London, 1959, p 256.